Shock Control Bumps for Mitigation of Transonic Buffet Loads on an Airfoil

Alessandro D'Aguanno[1,*], Alessandro Corduas[1], Ferry F. J. Schrijer[1] and Bas W. van Oudheusden[1]
1: Dept. of Flow Physics and Technology, Delft University of Technology, The Netherlands
* Corresponding author: alessandrodaguanno1@gmail.com
Keywords: Shockwave control, Transonic buffet, PIV, Pressure reconstruction, Supercritical airfoil

ABSTRACT Transonic buffet consists in the oscillation of a shockwave on the suction side of a wing/airfoil for a specific range of Ma, α and Re. To reduce this undesirable phenomenon, a passive control system has been experimentally investigated in this study: a shock control bump (SCB, see Bruce et al., 2015). Although several studies suggest that SCBs are effective in reducing transonic buffet oscillations (Giannelis et al., 2017), their effect on the mean flow and aerodynamic loads still has to be quantified. In this experimental study, three-dimensional SCBs have been applied on the suction side of an OAT15A supercritical airfoil (with chord, c=10 cm) with the experiments conducted in the transonic-supersonic wind tunnel of TU Delft at fully developed buffet conditions (Ma=0.7, α=3.5° and $Re=2.6\cdot10^6$, see D'Aguanno et al., 2021). The selected SCBs have a narrow wedge shape (Fig. 1, left) and are characterized by a flat ramp, crest and tail and by angular side flanks.
The effectiveness of the SCBs for different spanwise array spacings (ranging from 20%c to 30%c) was verified using two optical techniques: schlieren visualization and particle image velocimetry (PIV). Schlieren and PIV (see Fig. 1, right and Fig. 2, left) fields highlighted the presence of a λ-shock structure, which replaced the traditional quasi-normal shockwave in the presence of SCBs. A dedicated PIV investigation in a spanwise-chordwise measurement plane was conducted to characterize the effect of the spatial distribution of the bumps, focusing on the interaction of the shockwave structures along the span (see Fig. 2, right). The configuration with a spacing of Δy_{SCB} = 25%c was the most efficient in reducing transonic buffet oscillations, with a 34% reduction in the standard deviation of the shock position compared to the clean configuration. This also resulted in a reduction of the power spectral density at the buffet frequency (160 Hz) for the controlled configurations (see Fig. 3, right). In addition to stabilizing the shock position, SCBs reduced the pulsation and average extent of the separated area (the latter by 14%) compared to the clean configuration. Therefore, properly spaced SCBs demonstrate to be effective in both their possible working principles: shockwave stabilization and reduction of the separated area thanks to the vortex development from the SCBs side flanks.
The mean aerodynamic loads were reconstructed from low-speed planar PIV velocity data collected for the best-performing SCB configuration (Δy_{SCB} = 25%c) in a further experimental campaign. For lift evaluation, the pressure field was obtained using the integration procedure of van Oudheusden et al. (2007), while drag was calculated from the momentum deficit in the wake (Ragni et al., 2009). To account for spanwise load variation for the SCB configuration, PIV measurements were repeated at three different spanwise planes: along the centerline of the central bump (y/c = 0); at $y/c = \Delta y_{SCB}/4$; and at $y/c = \Delta y_{SCB}/2$. The average streamwise velocity field is shown in Fig. 2 (left) for the y/c = 0 SCB case. Fig. 3 (left) shows the shockwave position distribution for the SCB configuration (in the three measurement planes) and the clean configuration, confirming a clear reduction in oscillation range with SCBs. At the centerline of the SCB (y/c = 0), the range is wider and more upstream, while it is reduced at more outboard locations. Four buffet phases were defined according to the extent of the separated area and shock position: in its most upstream position (1); during the downstream movement (2); in the most downstream position (3); and while moving upstream (4).
Regarding the loads evaluation, the average value of the lift coefficient (C_l) is increased in presence of SCBs (of 4%), while an opposite trend is present for the drag coefficient (C_d) (reduction of 17%). Fig. 4, which compares the loads for the SCB case (average value of loads in the three measurement planes) and the clean configuration, clarifies that that the implementation of SCBs brings to a 70% reduction of the amplitude of oscillation for the lift coefficient and 40% for C_d. This aspect is particularly relevant, because of the direct positive influence it has on the fatigue life of an aerodynamic-structure undergoing buffet.

REFERENCES

Bruce, P.J.K., & Colliss, S.P. (2015). Review of research into shock control bumps. Shock Waves, 25(5):451–471.
D'Aguanno, A., Schrijer F.F.J., & van Oudheusden B.W. (2021). Experimental investigation of the transonic buffet cycle on a supercritical airfoil. Experiments in Fluids, 62, 214.
Giannelis, N., Vio, G., & Levinski, O. (2017). A review of recent developments in the understanding of transonic shock buffet. Progress in Aerospace Sciences, 92:39–84.
Ragni, D., Ashok, A., van Oudheusden, B., & Scarano, F. (2009). Surface pressure and determination of a transonic aerofoil based on particle image velocimetry. Measurement Science and Technology, 20.
van Oudheusden, B., Scarano, F., Roosenboom, E., Casimiri, E., & Souverein, L. (2007). Evaluation of integral forces and pressure fields from planar velocimetry data for incompressible and compressible Flows. Experiments in Fluids, 43:153-162.

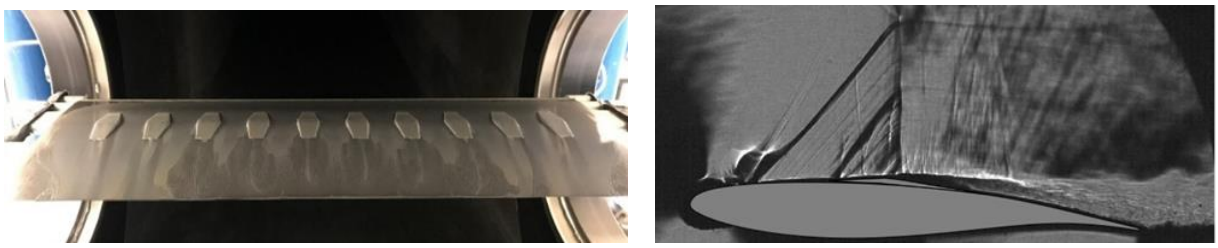

Figure 1. Wedge SCBs (Δy_{SCB}=25%c) on OAT15A airfoil (left) and corresponding instantaneous schlieren image (right).

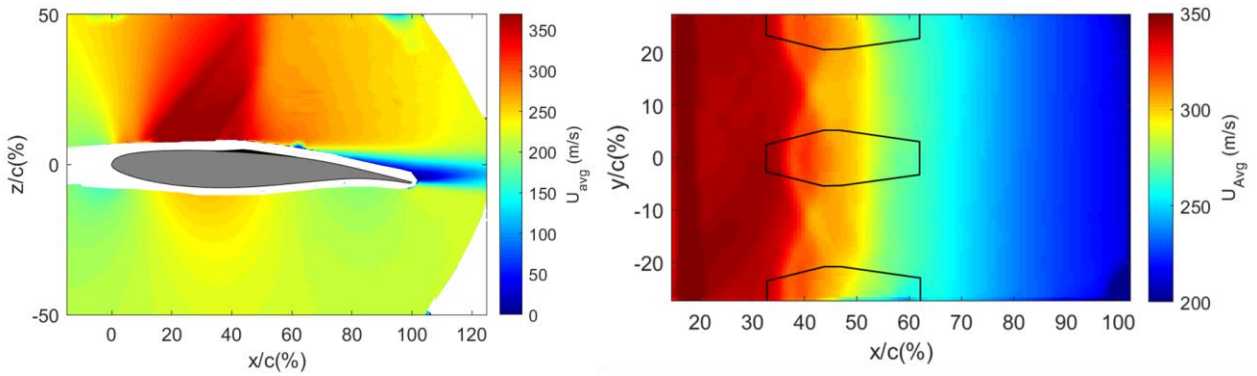

Figure 2. PIV streamwise avearge velocity field in the x-z (left) and in the x-y (right) planes.

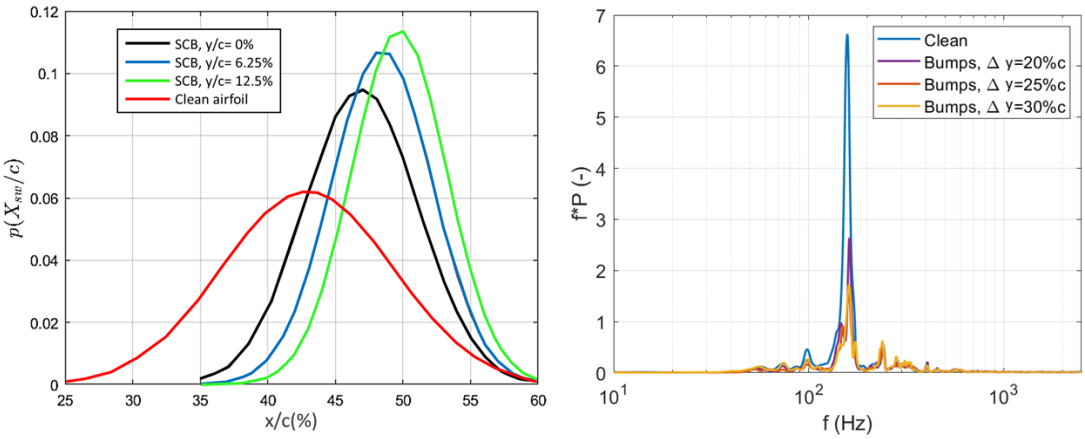

Figure 3. Left: Probability density function of shockwave distribution at different spanwise locations. Right: Power spectral density of shockwave position for different SCB spacings.

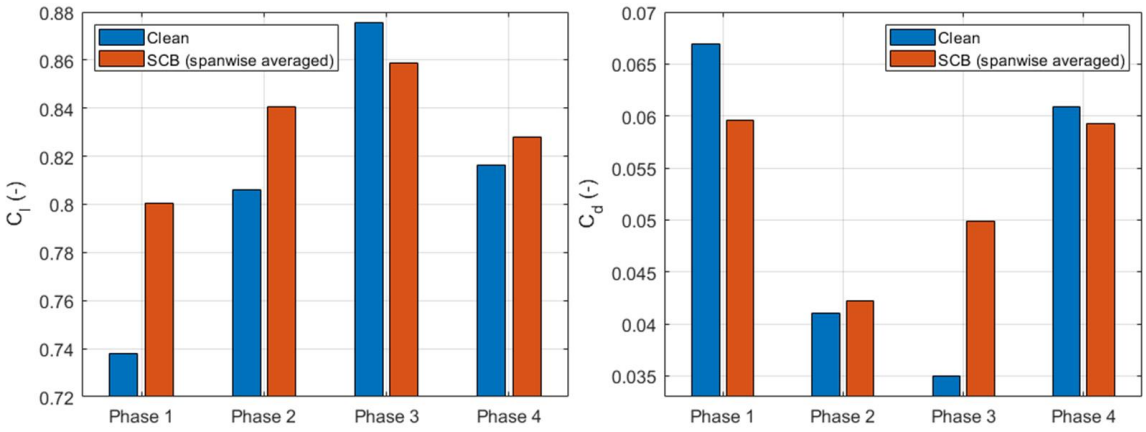

Figure 3. Lift (left) and drag (right) coefficients for the clean and the SCB configuration. The SCB data are here obtained by averaging the results in the three measurement planes (y/c=0; 6.25; 12.5%).